Thermochimica Acta 566 (2013) 57–70

Contents lists available at SciVerse ScienceDirect

Thermochimica Acta

journal homepage: www.elsevier.com/locate/tca

Crystallization kinetics and melting behaviors of poly(L-lactide)/graphene oxides composites

Hai-ming Chen, Wen-bin Zhang, Xue-chong Du, Jing-hui Yang, Nan Zhang, Ting Huang, Yong Wang*

Key Laboratory of Advanced Technologies of Materials (Ministry of Education), School of Materials Science & Engineering, Southwest Jiaotong University, Chengdu 610031, China

ARTICLE INFO

Article history:
Received 10 March 2013
Received in revised form 9 May 2013
Accepted 10 May 2013
Available online 18 May 2013

Keywords:
PLLA/GOs
Crystallization
Melting behavior

ABSTRACT

Poly(L-lactide)/graphene oxides (PLLA/GOs) composites containing different concentrations of GOs were prepared. Polarized optical microscope (POM) was used to characterize the isothermal crystallization morphologies of both neat PLLA and PLLA/GOs composites. Differential scanning calorimetry (DSC) was used to investigate the isothermal and nonisothermal crystallization and subsequent melting behaviors of the PLLA in different samples. Our results showed that GOs exhibited great role in improving the crystallization ability of the PLLA. During the isothermal crystallization process, addition of the only 0.1 wt% GOs accelerated the crystallization of the PLLA greatly. However, further increasing the concentration of the GOs was unfavorable for the crystallites perfection of the PLLA matrix, resulting in the decrease of equilibrium melting point accordingly. During the nonisothermal crystallization process, the crystallization behavior of the PLLA was found to be greatly dependent upon both the cooling rates and the concentration of the GOs. The corresponding crystallization kinetics was investigated and analyzed. Interestingly, it was observed that even if the cooling rate was increased up to 10 °C/min, the composites with high concentration of the GOs still show high crystallinity. This is very significant from a viewpoint of whether enhancing processing efficiency or preparing new PLLA material with excellent physical properties.

1. Introduction

Composites based on poly(L-lactide) (PLLA) attract much attention of many researchers because they exhibit interesting performance compared with neat PLLA. For example, with the presence of carbon nanotubes (CNTs) [1], exfoliated graphite [2] or silica (SiO_2) [3] in the PLLA matrix, largely improved thermal stability can be achieved for the composites. To improve the hydrolytic degradation ability of the PLLA, fillers such as clay or montmorillonite (MMT) [4], titanium dioxide (TiO_2) [5], CNTs [6–8] can be used. If conductive fillers such as CNTs and exfoliate graphite [2,9] are added, the PLLA composites also exhibit enhanced electrical conductivity. The high gas permeability of the PLLA can be decreased by adding MMT and graphene nanoplatelets [10,11] which have two dimensional sheet structure and increase the pathway length of gas molecules in the composites. Furthermore, improved mechanical properties of the PLLA composites can also be achieved [12–14].

Besides the above mentions, the crystallization improvement of the PLLA matrix induced by fillers is one of the most important aspects. On one hand, crystalline structures including the degree of crystallinity (X_c) and the crystal form of the PLLA matrix greatly influence the thermal properties, mechanical properties, hydrolytic degradation ability and gas permeability of articles [6,10,15–18]; on the other hand, from a viewpoint of processing, improved crystallization ability of the PLLA matrix facilitates the enhancement of processing efficiency [19]. For PLLA, it is very difficult to crystallize during the common processing ways and usually it is in the amorphous state. Therefore, improving the crystallization ability of the PLLA as much as possible through adding fillers becomes very significant. In this condition, fillers exhibit a role of nucleating agent to reduce the nucleation activation energy and increase the nucleation density of the PLLA matrix during the crystallization process.

However, the crystallization improvement of the PLLA matrix is proved to be dependent upon the type of fillers. For example, Hwang et al. [20] studied the nonisothermal crystallization of the PLLA containing organically modified MMT (OMMT) and found that even if the content of the OMMT was increased from 2.0 to 10.0 wt%, the crystallization temperature (T_c) was only enhanced from 113.4 to 114.9 °C. Huang et al. [21] investigated the nonisothermal crystallization behavior of PLLA with nano- and micro-scale SiO_2 and found that the nanoscale SiO_2 particles promoted the heterogeneous nucleation to increase crystallization, but microscale one formed hindrance to retard crystallization. Pan et al. [22] introduced layered double hydroxides into the PLLA and found that although the crystallization rate of the PLLA was greatly enhanced, the T_c of matrix was not influenced apparently during the nonisothermal crystallization process. Due to their relatively larger specific area, CNTs have been proved to be a very efficient

* Corresponding author. Tel.: +86 28 87603042.
E-mail address: yongwang1976@163.com (Y. Wang).

0040-6031/$ – see front matter © 2013 Elsevier B.V. All rights reserved.
http://dx.doi.org/10.1016/j.tca.2013.05.018

nucleating agent for most of semicrystalline polymers. Hence, the effect of CNTs on crystallization behavior of the PLLA has also been widely investigated [23]. Similarly, the crystallization of the PLLA in the PLLA/CNTs composites is also dependent upon the dispersion state [24], the surface modification method [25–27] and the content of the CNTs [8,28,29]. Specifically, relatively high content of CNTs retards the crystallization of the PLLA matrix, leading to the decrease of T_c due to that the CNTs network structure prevents the growth of the PLLA crystallites [28].

As one of the new fillers developed in recent years, GOs attract much attention of many researchers due to that GOs exhibit many intriguing features. On one hand, they have the similar chemical structure to modified CNTs; on the other hand, the functional groups on the surface of the GOs facilitate the good dispersion of the GOs in the polar polymer matrix. Therefore, adding GOs into the PLLA is also interesting and needs to be investigated in detail. For example, Pinto et al. found that the incorporation of the GOs significantly improved the mechanical properties and reduced gas permeability of the PLLA/GOs film toward oxygen and nitrogen [11]. Shen introduced thermal reduced GOs into the PLLA and found that the composites exhibited excellent electrical conductivity [30]. However, many researches still focus on the role of the GOs in improving the crystallization ability of the PLLA matrix. For example, Sun and He [31] found that the incorporation of the GOs leaded to lower crystallization activation energy of stereocomplex and higher crystallinity in the PLLA/GOs composites. Furthermore, it was proved that the heterogeneous nucleation effect of the GOs was dependent on the crystallization conditions. Pinto et al. [11] also found that the incorporation of 0.4 wt% GOs induced the cold crystallization of solution casting the PLLA/GOs sample during the DSC heating process, while no crystallization was detected for the pure PLLA sample. More detailed work about the crystallization of the PLLA/GOs composites has been done by Wang and Qiu [32,33]. In their work, they proved that the incorporation of the GOs not only improved the cold crystallization of the PLLA from the amorphous state, leading to the decrease of cold crystallization temperature with increasing the GOs concentration relative to neat PLLA despite heating rate, but also improved the melt crystallization ability during the isothermal crystallization process. Specifically, they proved that the GOs concentration exhibited great effect during the crystallization process, both the nonisothermal crystallization peak temperature and the overall isothermal melt crystallization rate of the PLLA matrix first increased and then decreased with the increase of the GOs concentration from 0.5 to 2.0 wt%.

Although some work has been carried out to understand the crystallization improvement of the PLLA with the incorporation of the GOs, much work still needs to be done to further understand the crystallization kinetics of the PLLA/GOs composites under the different crystallization conditions. Specifically, less work has been done to explore the relationship between the crystallization behaviors and the subsequent melting behaviors of the PLLA/GOs composites. Therefore, in this work, we attempted to investigate the isothermal and nonisothermal crystallization kinetics of the PLLA/GOs composites with the variation of the GOs concentration from 0.1 to 2.0 wt%. The melting behaviors of different composites obtained through different crystallization processes were also investigated in detail.

2. Experimental

2.1. Materials

PLLA (2002D, with D-isomer content of 4.3%, molecular weight (M_w) of 2.53×10^5 g/mol, melt flow rate (MFR) of 4–8 g/10 min (190 °C/2.16 kg) and density of 1.24 g/cm^3) was purchased from NatureWorks®, USA. Graphite was obtained from Qingdao Heilong Graphite Co., Ltd.

Table 1
Sample notation and the compositions of the composites.

Samples	Weight fraction of GOs (%)	Corresponding volume fraction of GOs (%)
PLLA	0.0	0.00
PLLA/0.1GOs	0.1	0.06
PLLA/0.5GOs	0.5	0.31
PLLA/1GOs	1.0	0.62
PLLA/2GOs	2.0	1.24

2.2. Sample preparation

GOs were prepared in our laboratory according to Hummer's method [34] and the corresponding data of the GOs can be seen in our previous work [35]. After the modification, some functional groups including carboxyl and hydroxyl groups were introduced to the surface of the GOs. The weight fraction of functional groups of the GOs was about 34.59% measured by thermogravimetric analysis.

To insure the good dispersion of the GOs in the PLLA matrix, samples were prepared through a so called master batch dilution method. First, GOs and PLLA were dissolved in the dimethylformamide (DMF) to prepare the solution of the GOs/DMF and the PLLA/DMF, respectively; then the solution of the GOs/DMF and the PLLA/DMF was mixed together with stirring at 80 °C for 2 h; and then the mixture was dried at 100 °C for enough time until the solvent was removed completely. Finally, the master batch of the PLLA/GOs composite containing 5.0 wt% GOs was prepared. After that, the master batch was melt compounded with neat PLLA to prepare the objective nanocomposites. Both the neat PLLA and the PLLA/GOs master batch were dried at 80 °C for 4 h before melt compounding processing. The melt compounding of all composites was carried out in an internal mixer at the melt temperature of 185 °C and rotate speed of 60 rpm, and the mixing duration was 5 min. In this work, the weight fraction of the GOs in the composites was varied from 0.1 to 2.0 wt%. The sample notation of the composites and the compositions are listed in Table 1. To give a more realistic understanding about the PLLA that was replaced by the GOs, the corresponding volume fraction was also given.

2.3. Characterizations

The isothermal crystallization morphologies of the neat PLLA and the PLLA/GOs composites were characterized using a polarized optical microscopy (POM, XPN203E, China) with a hot-stage. Firstly, a sample of about 5 mg was heated to 190 °C and pressed to obtain a slice with a thickness of about 20 μm. The slice was then maintained at 190 °C for 3 min to erase the thermal and mechanical history. Secondly, the slice was transferred to the hot-stage with a setting temperature of 110 °C and maintained at this temperature for 1 h. The crystallization morphology of the sample was taken images using a digital camera.

The isothermal crystallization and subsequent melting behaviors of the neat PLLA and the PLLA/GOs composites were investigated using differential scanning calorimetry (DSC, PerkinElmer Pyris-1, USA). Sample was heated to 200 °C and maintained at this temperature for 3 min to erase the thermal history, then the sample was cooled down to a predetermined isothermal crystallization temperature (T_{c-I}) at the cooling rate of 100 °C/min, maintained at this temperature for enough time to insure the completion of the crystallization of sample, and then the sample was cooled down to room temperature. After each crystallization process, the sample was heated again to 200 °C at a heating rate of 10 °C/min to

investigate the corresponding melting behavior of composite. Furthermore, the melting behavior of the PLLA matrix was further investigated using a temperature-modulated DSC (TMDSC) Q200 (TA Instrument, the USA). It should be pointed out that except the heating rate during the second heating scan (2 °C/min) was different from the previous DSC measurement (10 °C/min), the first heating rate and subsequent cooling rate were completely same with those used in the previous DSC measurement. When the sample was heated at 2 °C/min, a temperature modulation was superimposed with amplitude of 0.5 °C in a period of 60 s.

For the nonisothermal crystallization and subsequent melting behaviors, the measurements were conducted on a Netzsch STA 449C Jupiter (DSC). The sample was also heated from 0 to 200 °C at the heating rate of 10 °C/min and maintained at 200 °C for 3 min to erase any thermal history, then the sample was cooled down to room temperature at desired cooling rate (1, 2, 5 and 10 °C/min). Similarly, after each nonisothermal crystallization process, the sample was also reheated to 200 °C at the heating rate of 10 °C/min to understand the corresponding melting behavior of composite. All the DSC measurements were carried out in nitrogen atmosphere, and the weigh of each sample was about 8 mg.

3. Results and discussion

3.1. Isothermal crystallization and melting behaviors

Fig. 1 shows the isothermal crystallization morphologies of the neat PLLA and the PLLA/GOs composites. Neat PLLA exhibits sporadic but regular spherulites with typical Maltese Cross, and the average diameter of spherulites is about 40–50 μm. But, the whole crystallization rate of the neat PLLA is relatively small, and even if the crystallization time is up to 1 h, one can see that the crystallization of the neat PLLA is still not finished. The presence of the GOs greatly changes the crystallization behavior of the PLLA matrix. First, the number of the spherulites is dramatically increased. Obviously, GOs as heterogeneous nucleating agent for the PLLA crystallization increase the nucleation density of the PLLA apparently. Second, the diameter of spherulites is greatly decreased due to the increase of nucleation density. Third, all the PLLA/GOs composites exhibit irregular spherulites and the typical Maltese Cross which is observed for the neat PLLA is completely disappeared. This means that the presence of the GOs prevents the perfection of the PLLA spherulites during the crystallization process. Furthermore, it should be strengthened that the nucleation effect of the GOs is dependent upon the concentration of the GOs in the composites. The higher the concentration of the GOs, the more apparent the nucleation effect of the GOs is. Specifically for the PLLA/2GOs sample, it is very difficult to differentiate the spherulites one by one.

The isothermal crystallization behaviors of the neat PLLA and the PLLA/GOs composites were further investigated using DSC. The DSC heat flow curves of all samples during the isothermal crystallization process are shown in Fig. 2. Because the crystallization of the neat PLLA is very difficult and long time is required for the PLLA crystallization at relatively high crystallization temperature (T_{c-I}), relatively lower T_{c-I} (102, 105, 108 and 110 °C) was selected for

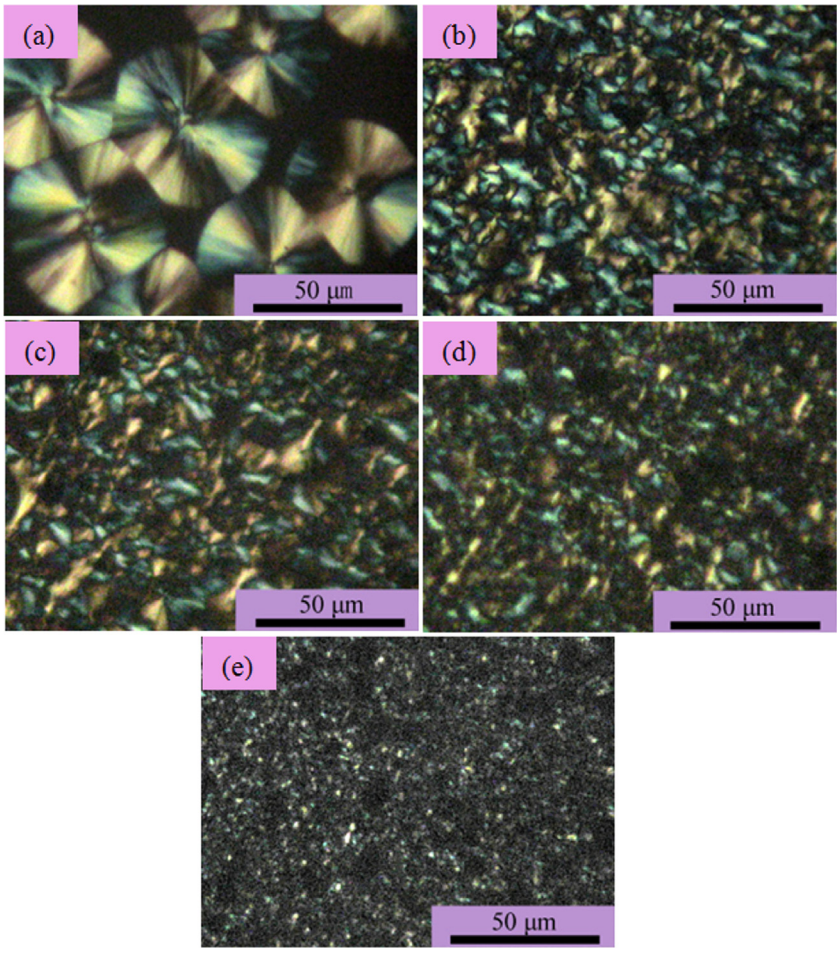

Fig. 1. POM images show the isothermal crystallization morphologies of different samples obtained after being crystallized at 110 °C for 1 h. (a) Neat PLLA, (b) PLLA/0.1GOs, (c) PLLA/0.5GOs, (d) PLLA/1GOs and (e) PLLA/2GOs.

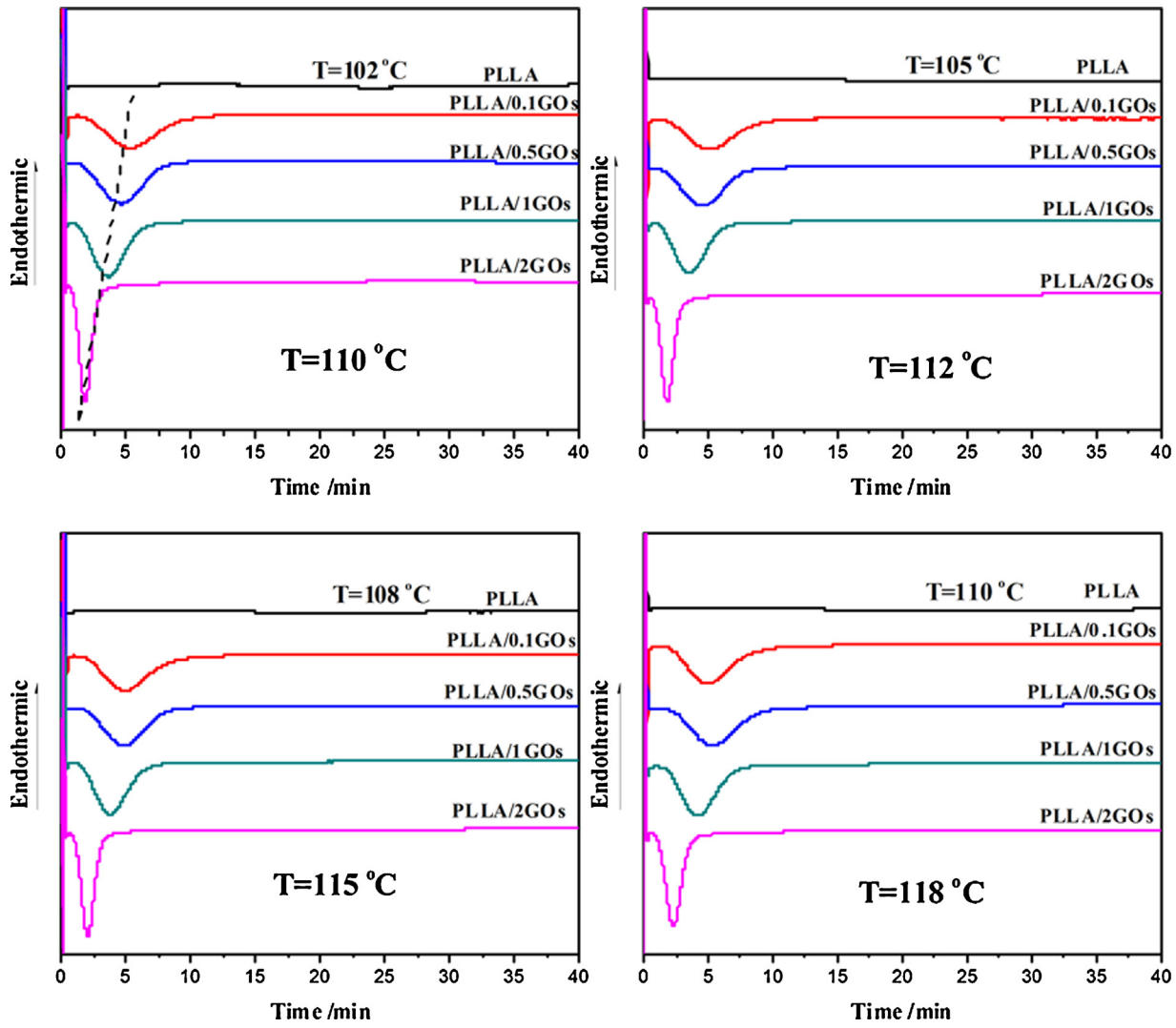

Fig. 2. DSC curves of neat PLLA and PLLA/GOs composites with different concentrations of GOs show the crystallization behaviors occurred at different isothermal crystallization temperatures as indicated in the graphs. For neat PLLA, the isothermal crystallization temperature is 102, 105, 108 and 110 °C, respectively.

the neat PLLA crystallization. For the PLLA/GOs composites, GOs exhibit great nucleation effect and the crystallization of the PLLA matrix is greatly accelerated as proved by previous POM characterization, therefore, relatively high T_{c-I} (110, 112, 115 and 118 °C) was selected. As shown in Fig. 2, at all crystallization temperatures, neat PLLA exhibits relatively lower crystallization process and the crystallization peak is broad and inconspicuous. However, all the PLLA/GOs composites exhibit relatively faster crystallization process even if the T_{c-I} selected for the PLLA/GOs composites is much higher than that for the neat PLLA. Generally, high crystallization temperature is unfavorable for the isothermal crystallization process of semicrystalline polymers since the formation of stable nucleus is relatively difficult. Here, even if the T_{c-I} is increased up to 118 °C, largely accelerated crystallization process is observed for the PLLA/0.1GOs sample compared with the crystallization process of the neat PLLA at T_{c-I} of 102 °C. Obviously, the positive effect of the GOs on the PLLA crystallization is over the negative effect of increasing crystallization temperature. Furthermore, it is observed that the heterogeneous nucleation effect of the GOs is very apparent and only 0.1 wt% GOs accelerate the isothermal crystallization process of the PLLA greatly. Further increasing the concentration of the GOs leads to the slightly decrease of time corresponding to the maximum crystallization rate. The relative crystallization fraction (X_t) evolution curves at different T_{c-I} are shown in Fig. 3. More apparently, the PLLA/GOs composites exhibit much bigger crystallization rate compared with the neat PLLA. In a very short time, the crystallization of the PLLA in the composites is finished. The higher the concentration of the GOs in the composites, the shorter the time required for the completion of crystallization.

The isothermal crystallization kinetics of semicrystalline polymers can be well described by the famous Avrami relation [36–38]:

$$1 - X_t = \exp(-Kt^n) \quad (1)$$

where X_t is the relative degree of crystallinity at crystallization time t, n is so called "Avrami exponent" which depends on the type of nucleation and the growth mechanism during the crystallization, and K is a rate constant related to nucleation and growth rate parameters. It should be pointed out that there is a presupposition that the type of crystallization does not change during the whole isothermal crystallization process and in this condition, the Avrami relation is valid in describing the crystallization kinetics of polymers. According to the Avrami equation, one formula can be got as follows:

$$\log[-\ln(1 - X_t)] = n \quad \log \quad t + \log \quad K \quad (2)$$

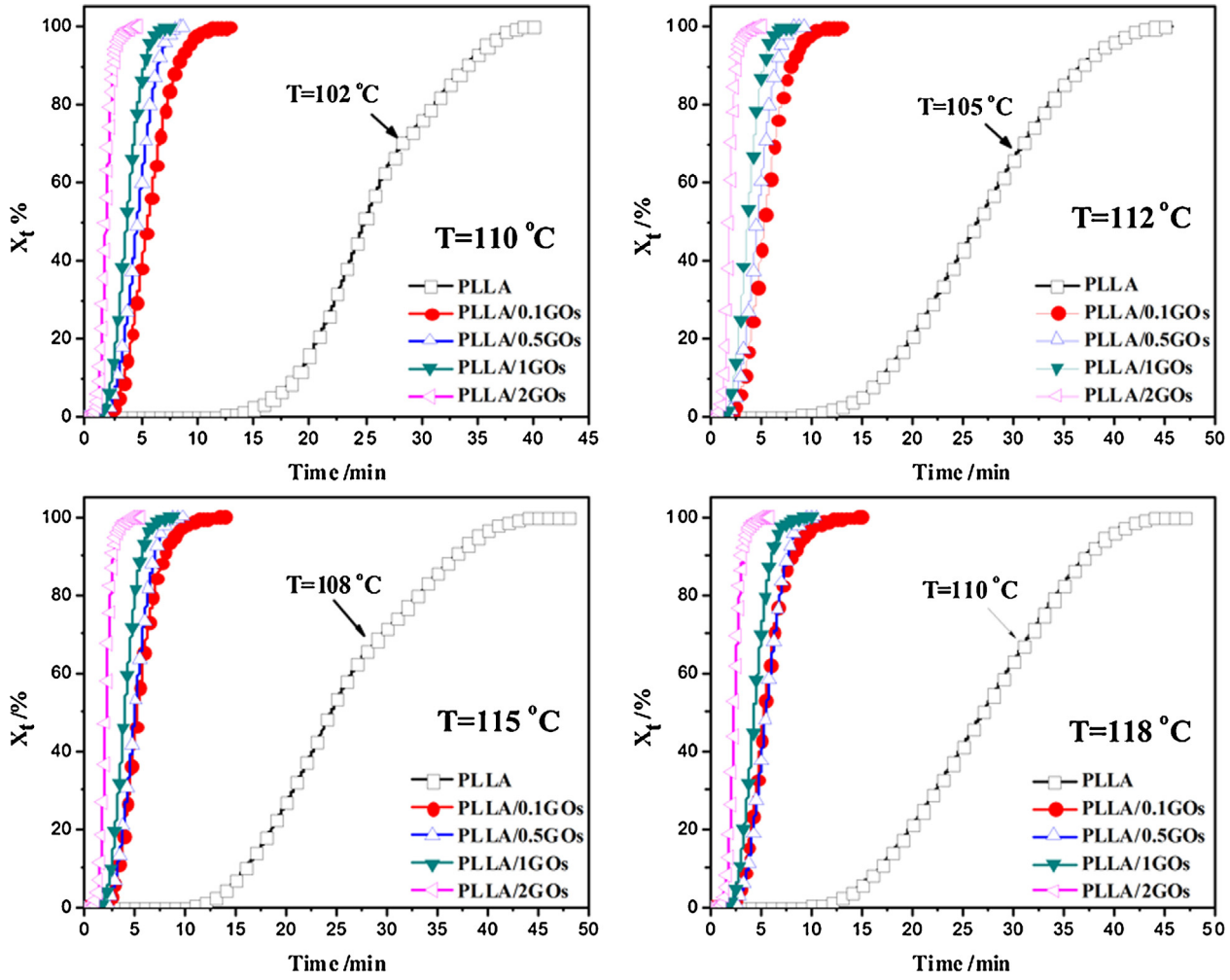

Fig. 3. Relative crystallization fraction versus crystallization time of neat PLLA and PLLA/GOs composites obtained at different isothermal crystallization temperatures as indicated in the graphs. The isothermal crystallization temperatures set for neat PLLA are also shown in the graphs.

And generally, the plot of $\log[-\ln(1-X_t)]$ versus $\log t$ provides a straight line. The slope of the line is n and the intercept with the ordinate yields $\log K$. Furthermore, from Eq. (1) the crystallization half time $t_{1/2}$ which is also used to describe the crystallization rate of polymers can be obtained by

$$t_{1/2} = \left(\frac{\ln 2}{K}\right)^{1/n} \tag{3}$$

The plots of $\log[-\ln(1-X_t)]$ versus $\log t$ of neat PLLA and PLLA/GOs composites are shown in Fig. 4 and the corresponding parameters for the isothermal crystallization kinetics are shown in Table 2. For the neat PLLA, only the crystallization behavior at T_{c-I} of 110 °C is comparatively analyzed. Obviously, for all the samples, the plots exhibit straight lines in the initial stage of the crystallization and then the slopes of the plots change slightly, indicating the variation of the crystallization behavior. This is possibly associated with the formation of new nucleus and the impingement of neighboring spherulites, and thus, represents beginning of the secondary crystallization. The variations of $t_{1/2}$ versus the concentration of GOs are illustrated in Fig. 5. Obviously, the PLLA/GOs composites exhibit much smaller $t_{1/2}$ compared with the neat PLLA although the crystallization temperatures set for the PLLA/GOs composites are much higher than that of the neat PLLA, indicating that GOs accelerate the isothermal crystallization process of the PLLA matrix greatly. Furthermore, there are at least two features which should be strengthened. First, for all the composites, although the T_{c-I} is increased from 110 to 118 °C, the $t_{1/2}$ changes slightly. For example, the $t_{1/2}$ of the PLLA/0.1GOs is increased from 5.1 min at T_{c-I} of 110 °C to 5.3 min at T_{c-I} of 118 °C. Second, the $t_{1/2}$ decreases with the increasing concentration of the GOs in the composites. This

Table 2
Isothermal crystallization kinetics parameters of neat PLLA and PLLA/GOs composites.

T_{c-I} (°C)	GOs content (wt%)	$t_{1/2}$ (min)	n	K
110	0.0	27.0	4.93	9.12E − 08
	0.1	5.1	4.46	4.17E − 04
	0.5	4.6	4.40	1.00E − 03
	1.0	3.6	4.63	2.14E − 03
	2.0	1.8	5.74	2.57E − 02
112	0.1	5.3	4.50	4.79E − 04
	0.5	4.6	4.57	7.76E − 04
	1.0	3.6	4.82	1.14E − 03
	2.0	1.9	5.83	2.19E − 02
115	0.1	5.5	4.72	3.89E − 04
	0.5	4.9	4.94	3.55E − 04
	1.0	3.8	5.07	9.55E − 04
	2.0	2.0	5.94	1.26E − 02
118	0.1	5.3	4.99	2.24E − 04
	0.5	5.1	5.34	1.02E − 04
	1.0	4.3	5.34	3.63E − 04
	2.0	2.4	5.88	5.37E − 03

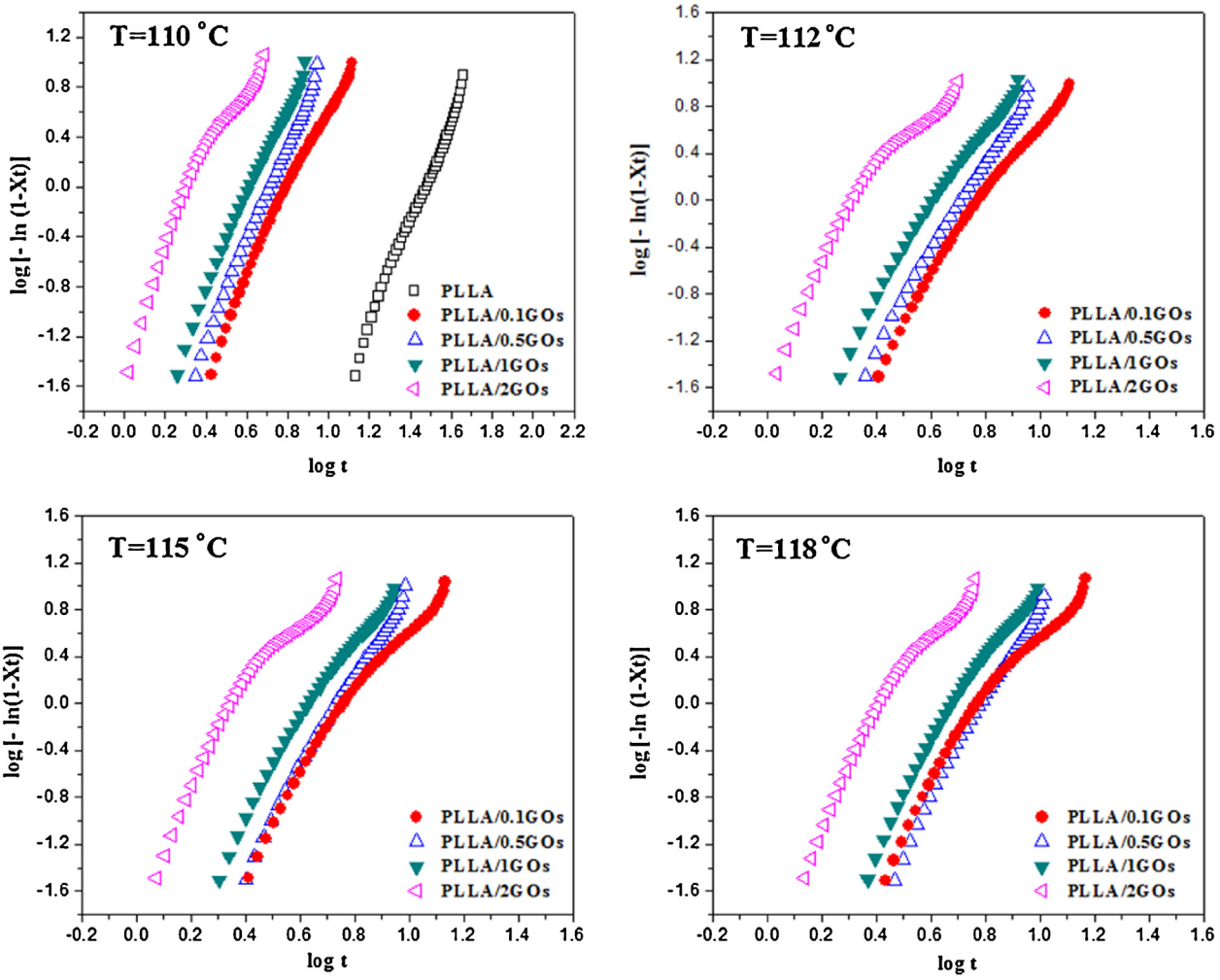

Fig. 4. Avrami plots of $\log[-\ln(1-X_t)]$ versus $\log t$ of neat PLLA and PLLA/GOs composites obtained at different isothermal crystallization temperatures as indicated in the graphs.

indicates that under the isothermal crystallization condition set in this work, the crystallization behavior of the PLLA in the composites is mainly determined by the concentration of GOs rather than the isothermal crystallization temperatures. As shown in Table 2, for all the samples, the Avrami exponent n is much larger than 3. It is also larger than the values reported in the literatures [39] in which the n is in the range of 2.1–2.5. The crystallization kinetics of the PLLA induced by nucleating agent investigated in our previous work [40] also given the similar values of n to those obtained in this work. Therefore, it is believed that the main reasons for the differences are mainly ascribed to the differences in both crystallization temperatures and the raw materials, which possibly induce the increase of crystal defect during the crystallization process. The variation trend of rate constant K also proves the accelerated crystallization process of the PLLA matrix induced by the GOs. The higher the concentration of the GOs in the composites, the bigger the K is.

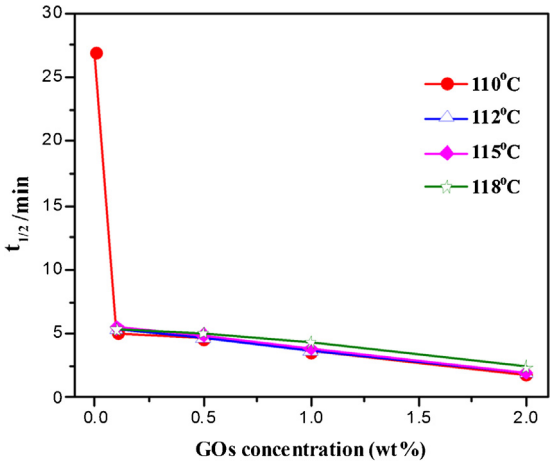

Fig. 5. Variation of crystallization half time versus the concentration of GOs in the composites.

The activation energy of nucleation (K_g) can be calculated according to the famous Hoffman–Lauritzen model [41]:

$$G = G_0 \exp\left[\frac{-U^*}{R(T_c - T_\infty)}\right] \exp\left[\frac{-K_g}{T_c \cdot \Delta T \cdot f}\right] \quad (4)$$

$$\ln G + \frac{U^*}{R(T_c - T_\infty)} = \ln G_0 - \frac{K_g}{T_c \cdot \Delta T \cdot f} \quad (5)$$

where G_0 is a constant independent of temperature; U^* represents the activation energy characteristic of the transport of the crystallizing segments across the liquid-crystal interface, universally $U^* = 6280$ J/mol; R is the gas constant; T_c is the isothermal

crystallization temperature; T_∞ is the theoretical temperature below which all motions associated with the viscous flow ceases, and generally, it is defined as $T_\infty = T_g - 30$ K; ΔT is the supercooling degree ($\Delta T = T_m^0 - T_c$), here T_m^0 is the equilibrium melting point which can be calculated according to the following equation (6); f is a corrective factor responsible for the variation of the equilibrium melting enthalpy with temperature, and it is defined as $f = 2T_c/(T_m^0 + T_c)$; and K_g is nucleation parameter. From Eq. (5), the slope of the plot of $\ln G + U^*/R(T_c - T_\infty)$ versus $1/T_c \cdot \Delta T \cdot f$ is K_g. Fig. 6 shows the plots of $\ln G + U^*/R(T_c - T_\infty)$ versus $1/T_c \cdot \Delta T \cdot f$ for the neat PLLA and the PLLA/GOs composites. The corresponding data of K_g are also shown in the graph. It can be seen that addition of only 0.1 wt% GOs induces the great decrease of K_g, further proving the good nucleation effect of the GOs for the PLLA matrix. For the PLLA/0.5GOs sample, the K_g is the smallest one. Further increasing the concentration of the GOs in the composites induces the slight increase of K_g, indicating that the nucleation effect of the GOs is decreased. However, it should be noticed that the value of K_g of the PLLA/2GOs samples is still much smaller than that of the neat PLLA.

The subsequent melting behaviors of samples are shown in Fig. 7. Similarly, for the neat PLLA, only the sample obtained after being isothermally crystallized at 110 °C is analyzed and the

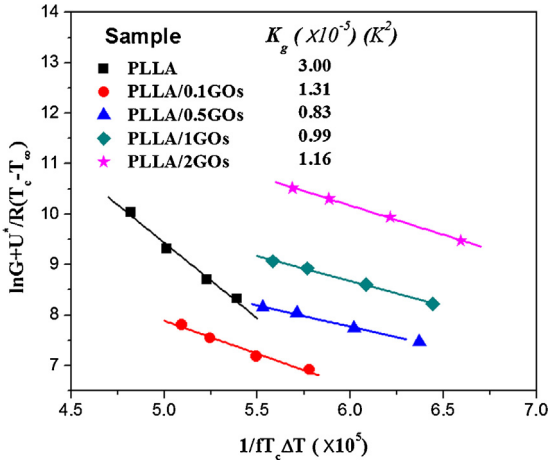

Fig. 6. Plots of $\ln G + U^*/R(T_c - T_\infty)$ versus $1/T_c \cdot \Delta T \cdot f$ for the neat PLLA and the PLLA/GOs composites.

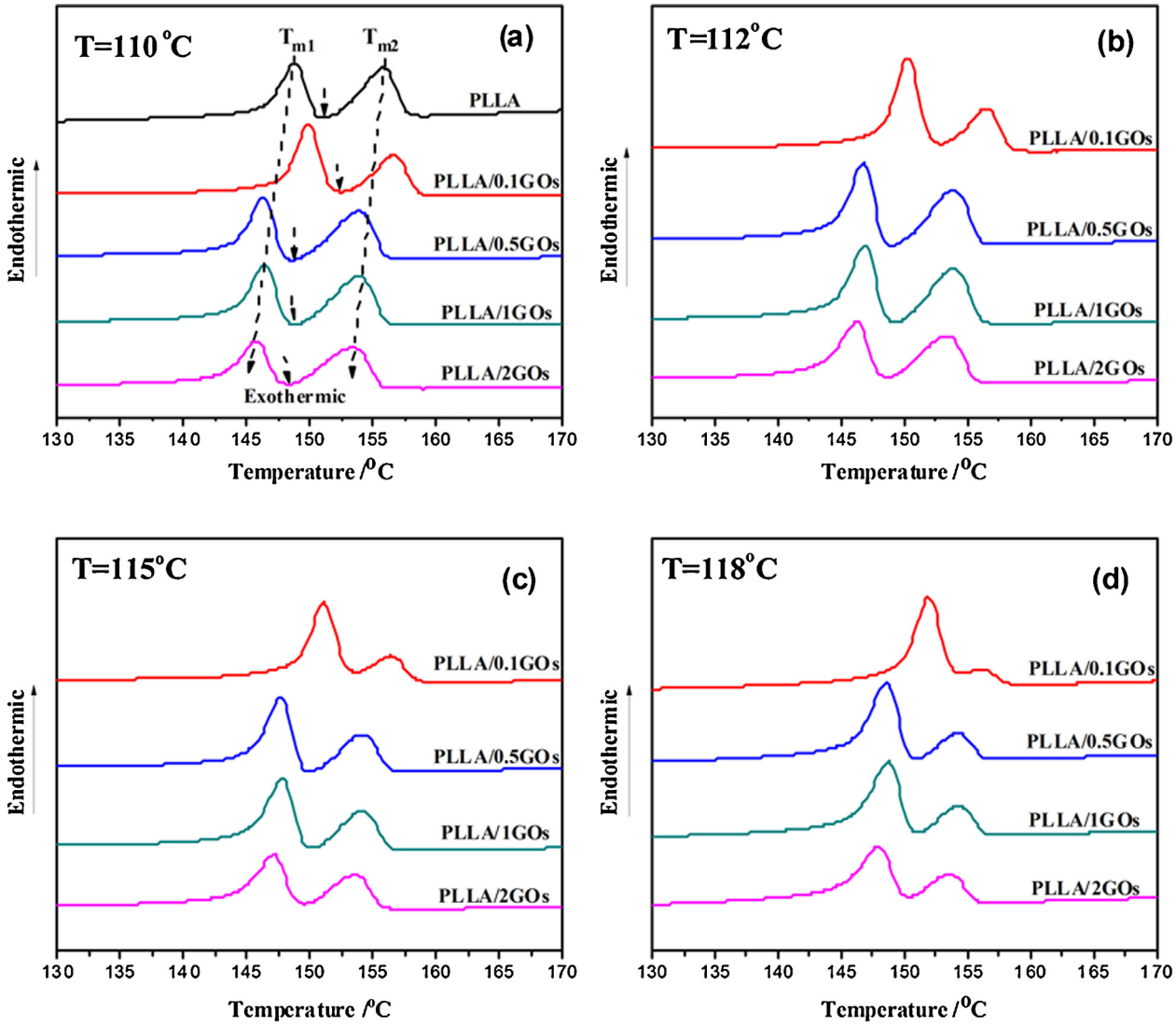

Fig. 7. DSC heating curves of neat PLLA and PLLA/GOs composites with different concentrations of GOs, recorded at a heating rate of 10 °C/min after isothermal crystallization at the temperatures indicated: (a) 110 °C, (b) 112 °C, (c) 115 °C and (d) 118 °C.

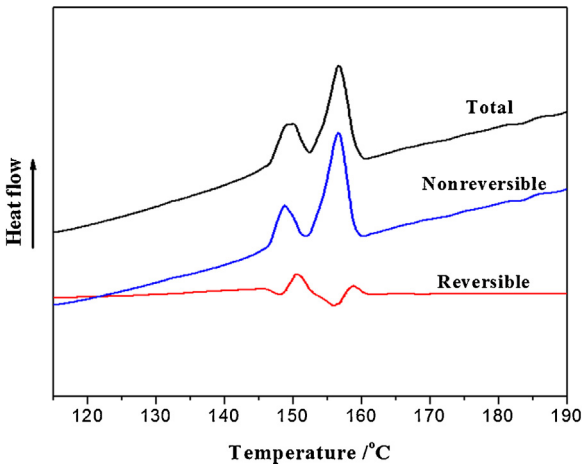

Fig. 8. TMDSC heat flow curves of the neat PLLA obtained at the heating rate of 2 °C/min. Sample was first crystallized at 110 °C.

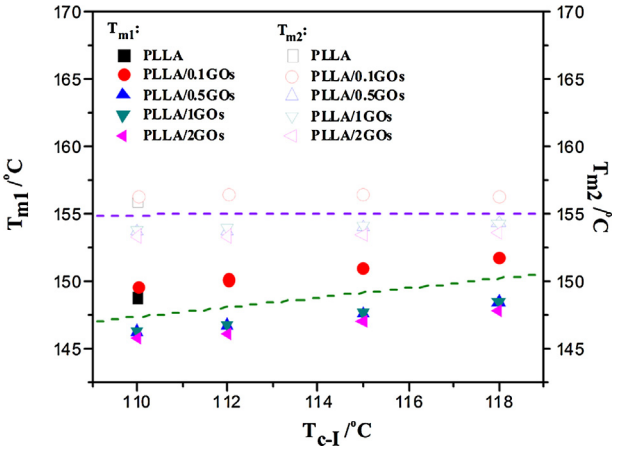

Fig. 9. Variations of melting temperatures (T_{m1} and T_{m2}) versus isothermal crystallization temperatures of neat PLLA and PLLA/GOs composites.

corresponding DSC heating curve is shown in Fig. 7a. After being isothermally crystallized 110 °C (Fig. 7a), it can be seen that all the samples exhibit double endothermic peaks on the DSC heating curves, attributing to the two different melting behaviors of the PLLA crystallites. For the neat PLLA, the first endothermic peak (T_{m1}) is at 148.7 °C and the second one (T_{m2}) at 155.9 °C. The presence of GOs induces the different variation trends of melt behaviors of the PLLA matrix. The PLLA/0.1GOs sample exhibits larger T_{m1} and T_{m2} compared with the neat PLLA. It is well known that the melting point is directly related to the thickness of lamellae and generally, the bigger the lamellar thickness, the higher the melting point is. Therefore, it can be deduced that addition of only 0.1 wt% GOs facilitates the perfection of crystalline structure of the PLLA matrix during the isothermal crystallization process. Further increasing the concentration of the GOs leads to the decrease of both T_{m1} and T_{m2}. The higher the concentration of GOs, the smaller the T_{m1} and T_{m2} are. This indicates that the presence of high concentration of the GOs is unfavorable for the perfection of the PLLA crystallites and contrarily, it endows PLLA crystallites with more defects. The similar melting behaviors of the PLLA/GOs composites are also observed by changing the crystallization temperatures, as shown in Fig. 7c–d. Furthermore, it is interesting to observe that the intensity of the first endothermic peak increases whereas the second endothermic peak weakens with the increase of T_{c-I}.

To further understand the mechanism for the double endothermic peaks observed for the neat PLLA and PLLA/GOs composites, the melting behavior of representative sample, i.e. the neat PLLA, was further investigated using TMDSC and the heat flow curves are shown in Fig. 8. Generally speaking, if the crystallization and melting occur simultaneously during the heating scan, the crystallization and melting signals can be separated in the reversible and non-reversible heat flow signals by TMDSC, respectively. As shown in Fig. 8, the total heat flow of the isothermal crystallized PLLA sample is separated in the endothermic heat flow signal attributing to the melt of PLLA crystallites (appearing in the non-reversible heat flow curve) and the exothermic heat flow signal attributing to the recrystallization (appearing in the reversible heat flow curve). This indicates the occurrence of the melt-recrystallization-melt process of the PLLA crystallites during the heating scan. Most likely, some crystallites formed during the isothermal crystallization process have imperfect crystalline structure and melt at relatively low temperature, and then the chain segments further crystallize and form the crystalline structures with thicker lamella. The latter lamella then melts at relatively higher temperatures. The similar results have been also reported in the literatures [42].

The variations of both T_{m1} and T_{m2} of different samples versus T_{c-I} are illustrated in Fig. 9. For a certain sample, T_{m1} increases with increasing T_{c-I} while T_{m2} maintains invariant, further proving that T_{m1} is related to the fusion of primary crystallites formed during the isothermal crystallization process while T_{m2} to the fusion of new crystallites formed during the DSC heating process through the melt–recrystallization–melt process of primary crystallites. For samples with different concentrations of the GOs, both T_{m1} and T_{m2} are observed to be dependent upon the concentration of the GOs in the composites. At all crystallization temperatures, the PLLA/0.1GOs sample exhibits the biggest T_{m1} and T_{m2}. However, increasing the concentration of the GOs induces the decrease of both T_{m1} and T_{m2}. Specifically, at all crystallization temperatures, the PLLA/2.0GOs sample exhibits the smallest T_{m1} and T_{m2}, and the data are even lower than those of the neat PLLA.

To further investigate the crystalline structures formed during the isothermal crystallization process, the typical equilibrium melting point (T_m^0) of the neat PLLA and the PLLA/GOs composites are calculated according to Hoffman–Weeks theory [43]:

$$T_m = \Phi T_{c-I} + (1 - \Phi)T_m^0 \quad (6)$$

where T_m is the observed melting point, T_{c-I} is defined as above, and Φ is the stability parameter depending on the crystal thickness. Generally, the crystal structure is very stable for $\Phi = 0$, and inherently unstable for $\Phi = 1$. The smaller the Φ value is, the more stable the crystal structure is. The T_m^0 values can be obtained by linear extrapolating the experimental data to $T_m = T_{c-I}$ line. In this work, the first endothermic peak (T_{m1}) was selected because it is directly related to the fusion of primary crystallites formed during the isothermal crystallization process. The results are illustrated in Fig. 10. Neat PLLA exhibits T_m^0 of 161.7 °C in this condition. Addition of only 0.1 wt% GOs dramatically improves the crystalline structure of the PLLA matrix and accordingly, the T_m^0 is increased up to 164.9 °C, indicating the formation of more perfect crystallites with bigger lamellar thickness. However, further increasing the concentration of the GOs induces the decrease of T_m^0. The higher the concentration of the GOs, the smaller the T_m^0 is. Obviously, high concentration of the GOs is unfavorable for the growth of the PLLA lamellae during the isothermal crystallization process.

It is well known to all that the effect of the filler on polymer crystallization is strongly affected by the shape and the concentration of the fillers in the composites. As reported by Li that the crystallization of polymer with the presence of nanofiller can be carried out through two possible routes [44]: homogeneous nucleation relating to the self-nucleation of the molecular chains away from

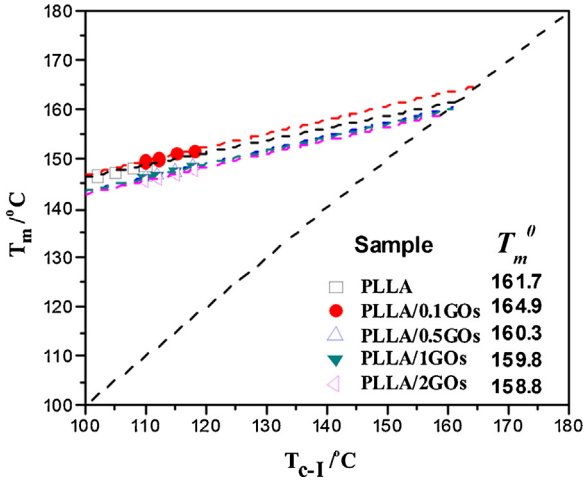

Fig. 10. Plots of melting temperature (T_{m1}) versus isothermal crystallization temperature for neat PLLA and PLLA/GOs composites.

the interface of the nanofiller and the polymer and heterogeneous nucleation relating to the nucleation of the molecular chains at the interface. High concentration of nanofiller provides larger surface area, facilitating the occurrence of the heterogeneous nucleation process. However, high concentration of nanofiller also hinders the diffusion of the molecular chains, leading to the decrease of the growth rate of lamellae. Therefore, the crystallization behavior should be the compromise between these two competing effects. In this work, with the presence of a few amounts of GOs, the functional groups on the surface of the GOs provide strong interfacial interaction with the molecular chains of the PLLA on one hand. On the other hand, the large surface of the GOs provides an ideal template for the molecular ordering of the molecular chains of the PLLA [45], facilitating the nucleation of the PLLA on the surface of the GOs accordingly. However, at high concentration of GOs, the diffusion of the PLLA molecular chains is restricted and the lamellar growth also occurs in a limited space, which is very similar to the crystallization of the PLLA in the nanocomposites with high concentration of carbon nanotubes [8,28,29]. Consequently, imperfect crystalline structures with smaller lamellar thickness are achieved.

3.2. Nonisothermal crystallization and melting behaviors

During the actual processing procedure, articles usually experience the nonisothermal crystallization process and therefore, it is very significant to investigate the nonisothermal crystallization behaviors of semicrystalline polymers. Fig. 11 shows the cooling traces of the neat PLLA and the PLLA/GOs composites obtained by DSC and the corresponding crystallization parameters are shown in Table 3. At all cooling rates ranging from 1 to 10 °C/min, no apparent exothermic phenomenon can be detected from the cooling curves of the neat PLLA, indicating that neat PLLA does not crystallize during the nonisothermal crystallization process. The presence of the GOs greatly improves the crystallization ability of the PLLA during the nonisothermal crystallization process; however, the crystallization behaviors of the PLLA/GOs composites are dependent upon the cooling rates. At cooling rate of 1 °C/min, all the composites exhibit the apparent crystallization behaviors of the PLLA matrix, and the crystallization peak temperature (T_c) increases with the increasing concentration of the GOs, further proving the great nucleation effect of the GOs on the PLLA crystallization. At cooling rates of 2 and 5 °C/min, although all the composites still show the crystallization behaviors of the PLLA matrix, it can be seen that the exothermic peaks of the PLLA/0.1GOs become inconspicuous compared with that obtained at cooling rate of 1 °C/min, indicating that fewer PLLA crystallizes during the cooling process. This can be further proved by the variation of crystallization enthalpy (ΔH_c) as shown in Table 3. When the cooling rate is increased up to 10 °C/min, only the PLLA/2GOs sample still shows the crystallization behavior. Generally, for a semicrystalline polymer with excellent crystallization ability, the exothermic phenomenon during the nonisothermal crystallization process becomes more apparent at relatively higher cooling rate. Such phenomenon can only be observed for the PLLA/2GOs sample in this work when cooling rate is increased from 1 to 5 °C/min. At cooling rate of 10 °C/min, although PLLA still crystallizes in the PLLA/2GOs sample, the ΔH_c (−22.4 J/g) is decreased compared with those (about −33 J/g) obtained at cooling rates ranging from 1 to 5 °C/min, further indicating that fewer PLLA crystallizes during the cooling process.

Similarly, the relative crystallization fraction (X_t) evolution curves at different cooling rates are illustrated and the results are shown in Fig. 12. Since neat PLLA does not show appar-

Table 3
Nonisothermal crystallization and subsequent melting parameters of neat PLLA and PLLA/GOs composites.

Cooling rate (°C/min)	GOs concentration (wt%)	T_c (°C)	ΔH_c (J/g)	T_g (°C)	T_{cc} (°C)	ΔH_{cc} (J/g)	T_m (°C)	ΔH_m (J/g)
1	0.0	–	–	60.5	122.9	−27.8	150.9/157.0	31.1
	0.1	118.1	−30.1	61.8	–	–	153.2	33.1
	0.5	119.5	−35.1	56.1	–	–	150.6/155.7	35.8
	1.0	120.6	−37.4	56.9	–	–	151.6/156.0	38.1
	2.0	124.0	−33.7	54.3	–	–	151.9/154.9	34.1
2	0.0	–	–	60.0	124.9	−29.5	151.4/157.0	29.3
	0.1	110.8	−28.6	61.4	–	–	150.9/155.7	31.1
	0.5	113.8	−35.4	55.9	–	–	148.4/155.7	34.8
	1.0	115.0	−37.2	56.7	–	–	149.4/156.0	37.5
	2.0	119.8	−32.7	53.8	–	–	144.9/155.2	34.8
5	0.0	–	–	59.4	125.8	−28.9	151.6/156.7	25.8
	0.1	99.9	−4.38	60.8	115.3	−20.1	149.9/155.7	37.1
	0.5	102.9	−17.4	56.3	108.9	−13.6	144.9/155.1	31.2
	1.0	104.2	−25.3	56.5	106.8	−8.6	145.8/155.0	33.5
	2.0	112.0	−33.1	54.2	–	–	147.1/155.2	33.0
10	0.0	–	–	59.1	126.4	−26.1	151.5/156.4	24.9
	0.1	–	–	60.3	115.2	−23.9	149.8/155.4	20.1
	0.5	–	–	57.0	112.9	−26.6	145.8/155.3	25.2
	1.0	–	–	57.1	111.0	−28.5	146.0/155.4	28.2
	2.0	102.1	−22.4	54.4	–	–	144.7/154.9	26.9

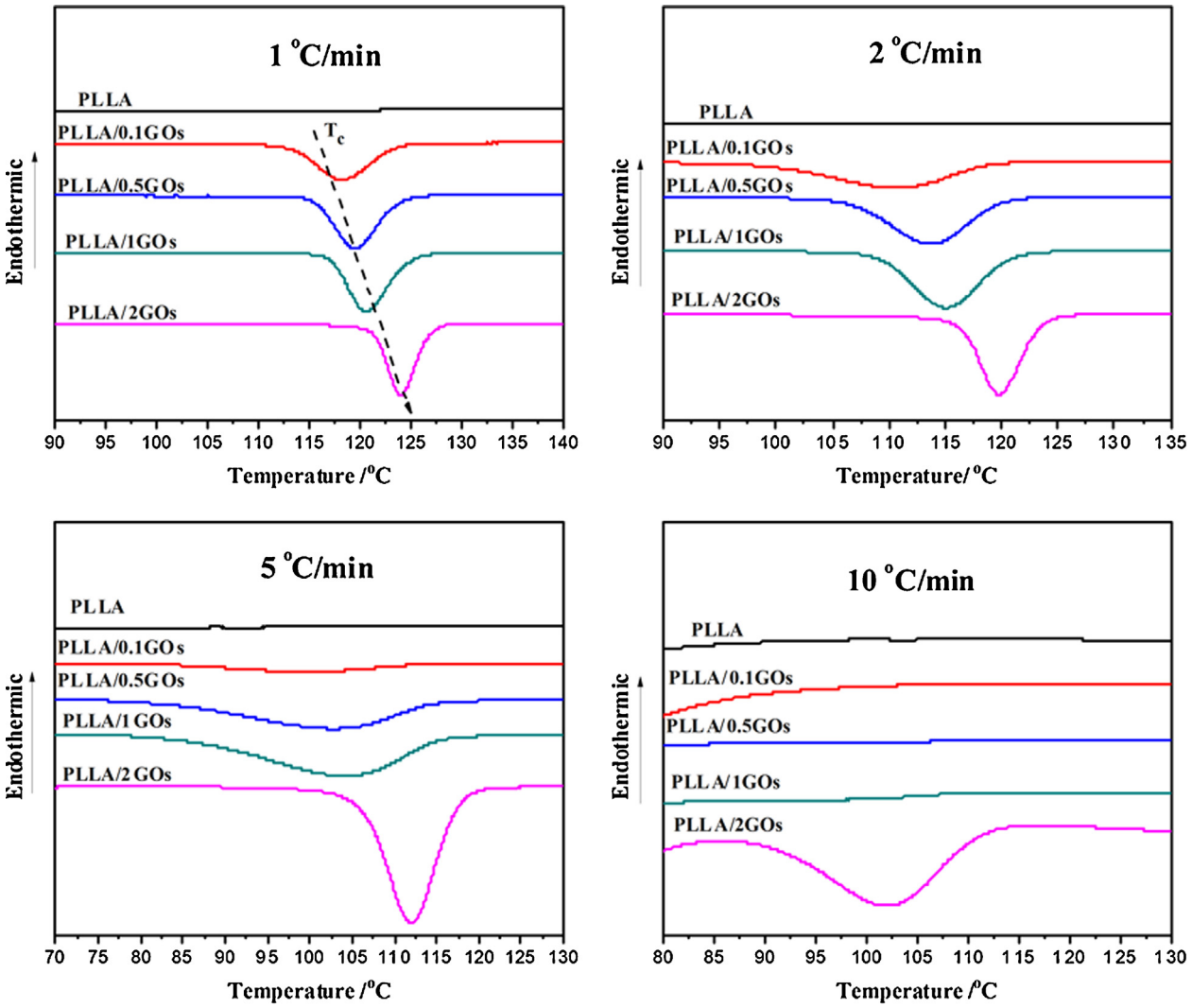

Fig. 11. DSC cooling curves show the nonisothermal crystallization behaviors of neat PLLA and PLLA/GOs composites obtained at different cooling rates as indicated.

ent crystallization behavior at all cooling rates selected in this work, therefore only the results of the PLLA/GOs composites are shown. Furthermore, the results obtained at cooling rate of 10 °C/min are not considered because only the PLLA/2GOs sample could exhibit the crystallization behavior under this condition. More apparently, the crystallization rate of the PLLA/GOs composites is greatly dependent upon the concentration of GOs. The more the concentration of GOs, the bigger the crystallization rate of PLLA matrix is. This agrees well with the observations obtained from isothermal crystallization process.

The nonisothermal crystallization kinetics of the PLLA/GOs composites can be described by Mo which combines the Avrami equation and Ozawa equation [46,47]:

$$\log \phi = \log F(T) - \alpha \log t \quad (7)$$

where ϕ is the cooling rate, the kinetic parameter $F(T)$ refers to the value of cooling rate that has to be selected at unit crystallization time when the sample has the defined degree of crystallinity; α is the ratio of the Avrami exponent n to the Ozawa exponent m. The plots of log ϕ versus log t are shown in Fig. 13, and the data of $F(T)$ and α obtained from the intercept and slope of the plots are shown in Table 4. From Fig. 13 one can see that for all the composites, the plots are straight lines, indicating that the nonisothermal crystallization kinetics of the PLLA/GOs composites can be well described by Mo method. Furthermore, the results shown in Table 4 suggest that at a certain crystallization time, a higher relative degree of

Table 4
Nonisothermal crystallization kinetics parameters of PLLA/GOs composites obtained by Mo method.

X_t (%)	GOs content (wt%)	$F(T)$	a
30	0.1	1.45	1.73
	0.5	1.49	1.94
	1.0	1.47	1.99
	2.0	1.22	2.00
40	0.1	1.67	1.90
	0.5	1.61	1.99
	1.0	1.60	2.06
	2.0	1.28	1.97
50	0.1	1.77	1.93
	0.5	1.81	2.15
	1.0	1.78	2.21
	2.0	1.34	1.98
60	0.1	1.90	2.00
	0.5	2.02	2.33
	1.0	1.96	2.33
	2.0	1.40	1.97

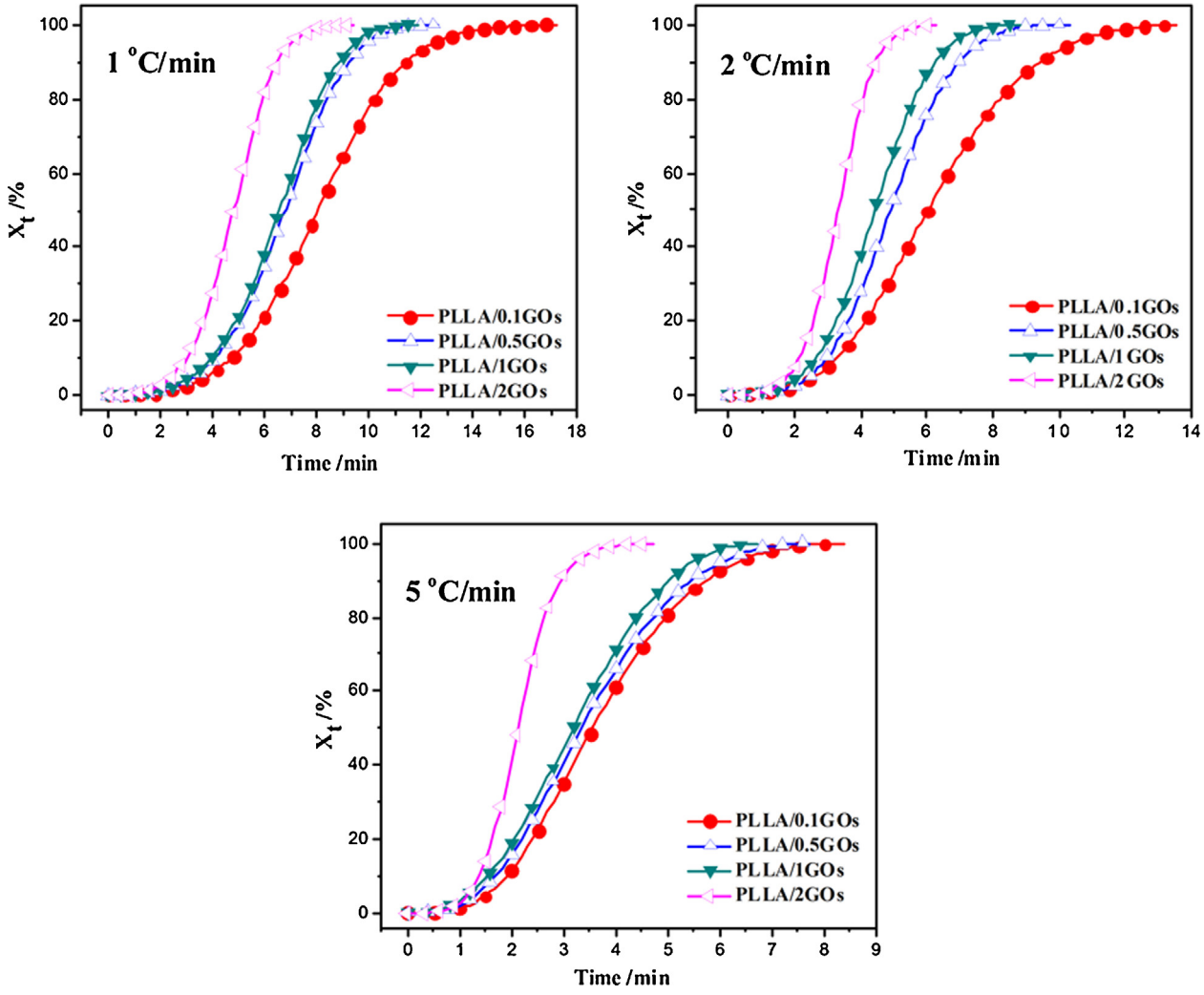

Fig. 12. Relative crystallization fraction versus crystallization time of PLLA/GOs composites obtained at different cooling rates as indicated.

crystallinity (X_t) can be obtained at a higher cooling rate. Furthermore, at a certain X_t, a lower cooling rate is required for sample with relatively higher concentration of GOs. The values of α changes slightly, further indicating that the nonisothermal crystallization process involving the nucleation and spherulites growth of the composites can be influenced by the concentration of the GOs.

The subsequent heating curves of different samples are shown in Fig. 14 and the corresponding parameters obtained from DSC curves are also shown in Table 3. From the heating curve of the neat PLLA which is first cooled from the melt at a cooling rate of 1 °C/min (Fig. 14a), one can see that there are several transitions, including the glass transition at 60.5 °C (T_g), the exothermic phenomenon attributed to the cold crystallization behavior of the PLLA at 122.9 °C (T_{cc}), and the endothermic phenomenon attributed to the melting of the PLLA crystallites at about 150.9 (T_{m1}) and 157.0 °C (T_{m2}). As shown in Fig. 11, neat PLLA does not crystallize apparently at all cooling rates. Therefore, the observed endothermic phenomenon originated from the fusion of PLLA crystallites which are induced during the DSC heating process through the cold crystallization occurred at 122.9 °C. With the increase of cooling rate, the T_{cc} of the neat PLLA shifts to higher temperatures. This can be explained by the variation of ordered structure in the sample. At relatively lower cooling rate, although PLLA does not crystallize, some PLLA macromolecules form the ordered structures through conformation adjustment, and these ordered structures act as a nucleus to promote the occurrence of the cold crystallization of the PLLA at relatively lower T_{cc} during the DSC heating process. The presence of ordered structure can also be proved by the weak endothermic peak rather than the common step change observed in the glass transition range. Increasing cooling rate leads to fewer ordered structures formation during the cooling process, and therefore it is more difficult for the occurrence of the cold crystallization of the neat PLLA.

For the PLLA/GOs composites, it can be seen that all the transitions are dependent upon the concentration of the GOs and the cooling rate. First, T_g of composites decreases with the increasing concentration of the GOs, indicating that high concentration of the GOs is favorable for the relaxation of the PLLA chain segments. This will be further discussed in our next work. Second, after being crystallized at relatively lower cooling rate, i.e. 1 and 2 °C/min, the cold crystallization process disappears completely, indicating that the crystallization of the PLLA matrix is finished during the cooling process; however, at cooling rate of 5 and 10 °C/min, the PLLA/0.1GOs, PLLA/0.5GOs and PLLA/1GOs samples exhibit the apparent cold crystallization behaviors. The T_{cc} shifts to lower temperatures with the increasing concentration of the GOs in the sample, and the data are much smaller than those of

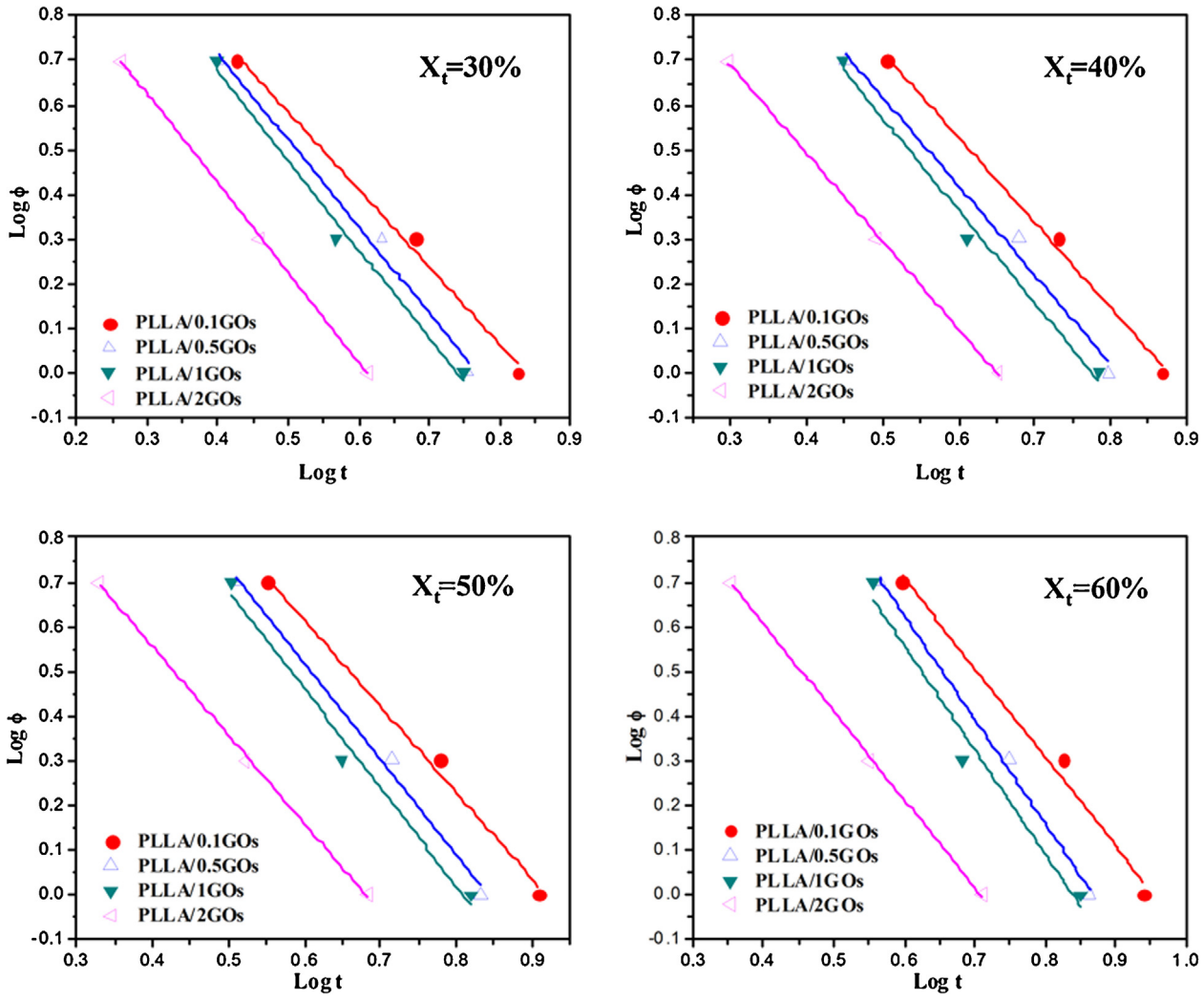

Fig. 13. Plots of log ϕ versus log t of PLLA/GOs composites with different concentrations of GOs at a certain relative crystallization fraction as indicated.

the neat PLLA. This indicates the heterogeneous nucleation effect of the GOs on cold crystallization of the PLLA on one hand. The more the concentration of the GOs, the more apparent the heterogeneous nucleation effect is. On the other hand, the presence of cold crystallization behavior also indicates the crystallization of the PLLA matrix is not finished during the cooling process. However, for the PLLA/2GOs sample, even if the cooling rate is increased up to 10 °C/min, the cold crystallization is still not observed, suggesting the completely completion of crystallization during the cooling process.

Furthermore, the melting behaviors of the PLLA in different samples also change with the variations of both cooling rate and the concentration of the GOs. On one hand, T_{m1} decreases with increasing concentration of GOs while T_{m2} maintains nearly invariant; On the other hand, relatively smaller cooling rate leads to higher T_{m1}. The results obtained from nonisothermal crystallization process are well consistent with those obtained from isothermal crystallization process, namely, the T_{m1} is mainly related to the fusion of primary crystallites formed during the nonisothermal crystallization process and/or cold crystallization process during the DSC heating and T_{m2} is related to the fusion of new crystallites formed through so called melt–recrystallize–melt process of imperfect crystallites.

The degree of crystallinity (X_c) of the PLLA is calculated according to the following equation:

$$X_c = \frac{\Delta H_m - \Delta H_{cc}}{\Delta H_M^0 \times \varphi} \times 100\% \quad (8)$$

where ΔH_m is the DSC measured value of fusion enthalpy, ΔH_{cc} is the cold crystallization enthalpy obtained during the DSC heating process, ΔH_m^0 is the fusion enthalpy of the completely crystalline PLLA, and φ is the weight fraction of PLLA in the sample. Here, the value of ΔH_m^0 of PLLA is selected as 93 J/g [48]. The data of ΔH_m and ΔH_{cc} are also shown in Table 3 and the variations of X_c versus the concentration of GOs are illustrated in Fig. 15. Obviously, the presence of the GOs greatly improves the crystallization ability of the PLLA and largely increased X_c is obtained at relatively lower cooling rate. Increasing the cooling rate is unfavorable for the crystallization improvement of the PLLA matrix. However, it can be seen that even if the cooling rate is increased up to 10 °C/min, the PLLA/2GOs sample still shows the X_c of 29.5%. In other words, the negative effect of increased cooling rate in the actual processing conditions on the crystallization of the PLLA can be eliminated by increasing the concentration of the GOs to a certain extent. Obviously, high crystallinity hints high thermal properties and high modulus and strength. This is very significant from viewpoints of enhancing

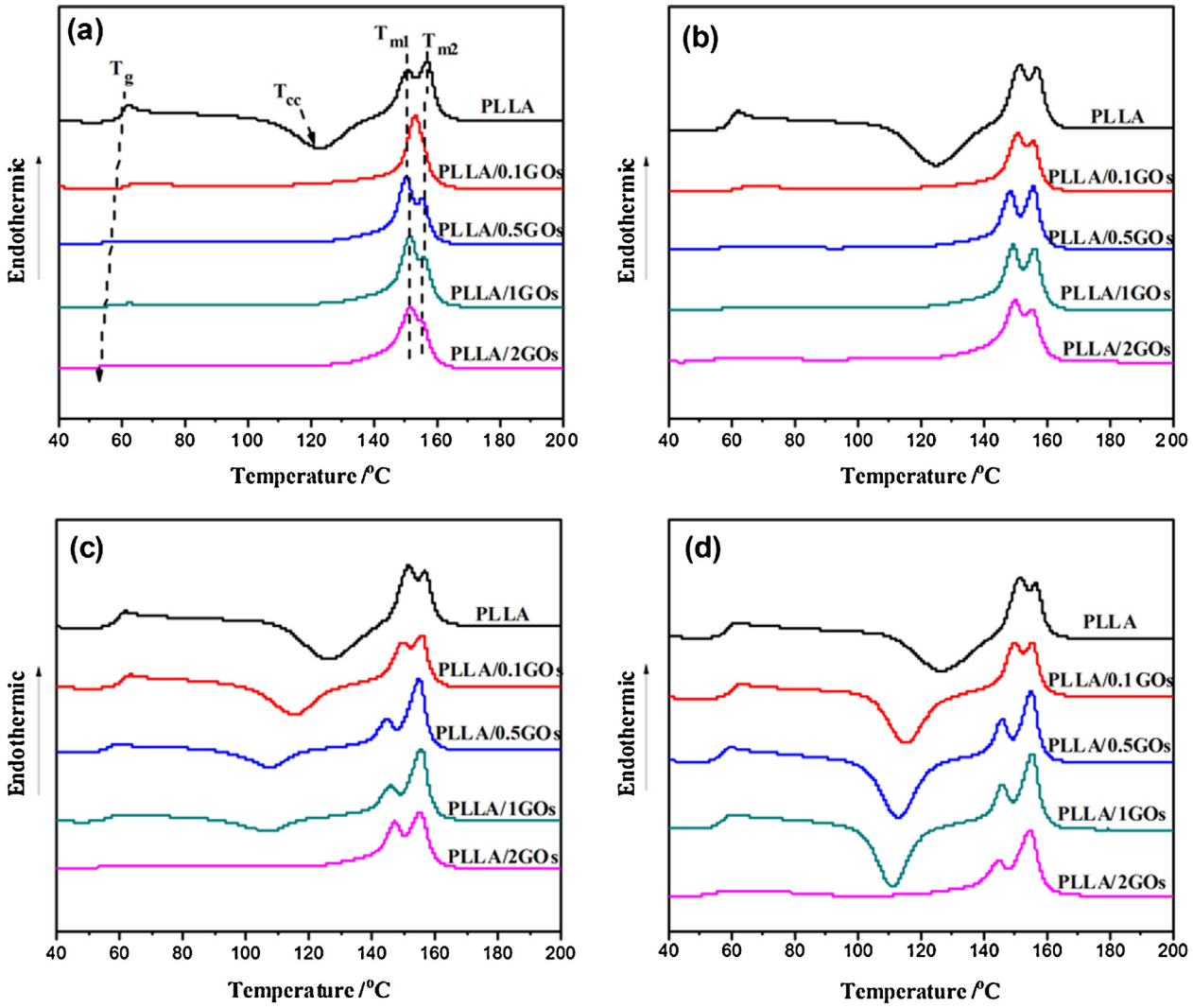

Fig. 14. DSC heating curves of neat PLLA and PLLA/GOs composites with different concentrations of GOs, recorded at a heating rate of 10 °C/min after being cooled at different cooling rates. (a) 1 °C/min, (b) 2 °C/min, (c) 5 °C/min and (d) 10 °C/min.

processing efficiency and preparing new PLLA material with excellent physical properties.

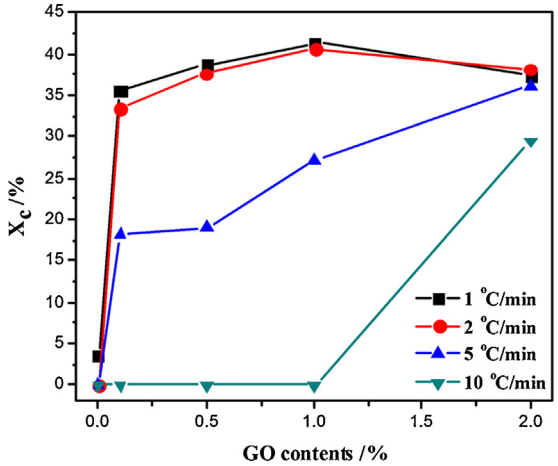

Fig. 15. Variations of crystallinity of neat PLLA and PLLA/GOs composites as the function of GOs concentration.

4. Conclusions

In summary, the isothermal and nonisothermal crystallization behaviors of the neat PLLA and the PLLA/GOs composites were comparatively investigated. It is found that GOs exhibit great role in improving the crystallization ability of the PLLA. During the isothermal crystallization process, addition of only 0.1 wt% GOs dramatically accelerates the crystallization of the PLLA matrix and the crystallization half time is dramatically decreased. Increasing the concentration of the GOs further accelerates the crystallization, but high concentration of the GOs is unfavorable for the crystal perfection of the PLLA, which can be proved by the decrease of equilibrium melting temperature. During the nonisothermal crystallization process, it is observed that the crystallization behavior of the PLLA is greatly dependent upon both the cooling rate and the concentration of the GOs. At relatively small cooling rate, the crystallization temperature of the PLLA increases with the increasing concentration of the GOs. At relatively high cooling rate, high concentration of the GOs is required to realize the crystallization of the PLLA. The most interesting is that even if the cooling rate is

increased up to 10 °C/min, the composites with high concentration of the GOs still show the high crystallinity.

Acknowledgments

Authors express their sincere thanks to the National Natural Science Foundation of China (51203129, 50973090), Distinguished Young Scholars Foundation of Sichuan (2012JQ0057) and the Fundamental Research Funds for the Central Universities (SWJTU12CX010, SWJTU11CX142, SWJTU11ZT10) for financial support.

References

[1] Z. Morávková, M. Trchová, E. Tomsík, J. Cechvala, J. Stejskal, Enhanced thermal stability of multi-walled carbon nanotubes after coating with polyaniline salt, Polym. Degrad. Stab. 97 (2012) 1405–1414.
[2] I.H. Kim, Y.G. Jeong, Polylactide/exfoliated graphite nanocomposites with enhanced thermal stability, mechanical modulus, and electrical conductivity, J. Polym. Sci., Part B: Polym. Phys. 48 (2010) 850–858.
[3] J. Zhang, J.Z. Lou, S. Ilias, P. Krishnamachari, J.Z. Yan, Thermal properties of poly(lactic acid) fumed silica nanocomposites: experiments and molecular dynamics simulations, Polymer 49 (2008) 2381–2386.
[4] H.M. Chen, J. Chen, J. Chen, J.H. Yang, T. Huang, N. Zhang, Y. Wang, Effect of organic montmorillonite on cold crystallization and hydrolytic degradation of poly(L-lactide), Polym. Degrad. Stab. 97 (2012) 2273–2283.
[5] Y.B. Luo, X.L. Wang, Y.Z. Wang, Effect of TiO2 nanoparticles on the long-term hydrolytic degradation behavior of PLA, Polym. Degrad. Stab. 97 (2012) 721–728.
[6] H.M. Chen, C.X. Feng, W.B. Zhang, J.H. Yang, T. Huang, N. Zhang, Y. Wang, Hydrolytic degradation behavior of poly(L-lactide)/carbon nanotubes nanocomposites, Polym. Degrad. Stab. 98 (2013) 198–208.
[7] Y.Y. Zhao, Z.b. Qiu, Wa.t. Yang, Effect of functionalization of multiwalled nanotubes on the crystallization and hydrolytic degradation of biodegradable poly(L-lactide), J. Phys. Chem. B 112 (2008) 16461–16468.
[8] Y.Y. Zhao, Z.B. Qiu, W.T. Yang, Effect of multi-walled carbon nanotubes on the crystallization and hydrolytic degradation of biodegradable poly(L-lactide), Compos. Sci. Technol. 69 (2009) 627–632.
[9] H. Quan, S.J. Zhang, J.L. Qiao, L.Y. Zhang, The electrical properties and crystallization of stereocomplex poly(lactic acid) filled with carbon nanotubes, Polymer 53 (2012) 4547–4552.
[10] E. Picard, E. Espuche, R. Fulchiron, Effect of an organo-modified montmorillonite on PLA crystallization and gas barrier properties, Appl. Clay Sci. 53 (2011) 58–65.
[11] A.M. Pinto, J. Cabral, D.A.P. Tanaka, A.M. Mendes, F.D. Magalhaes, Effect of incorporation of graphene oxide and graphene nanoplatelets on mechanical and gas permeability properties of poly(lactic acid) films, Polym. Int. 62 (2013) 33–40.
[12] J. Wootthikanokkhan, T. Cheachun, N. Sombatsompop, S. Thumsorn, N. Kaabbuathong, N. Wongta, J. Wong-On, S.I.N. Ayutthaya, A. Kositchaiyong, Crystallization and thermomechanical properties of PLA composites: effects of additive types and heat treatment, J. Appl. Polym. Sci. 129 (2013) 215–223.
[13] A. Pei, Q. Zhou, L.A. Berglund, Functionalized cellulose nanocrystals as biobased nucleation agents in poly(L-lactide) (PLLA) – crystallization and mechanical property effects, Compos. Sci. Technol. 70 (2010) 815–821.
[14] B. Li, F.X. Dong, X.L. Wang, J. Yang, D.Y. Wang, Y.Z. Wang, Organically modified rectorite toughened poly(lactic acid): nanostructures, crystallization and mechanical properties, Eur. Polym. J. 45 (2009) 2996–3003.
[15] D.F. Wu, L. Wu, W. Yu, B. Xu, M. Zhang, Degradation induced by nanostructural evolution of polylactide/clay nanocomposites in the isothermal cold crystallization process, Polym. Int. 58 (2009) 430–436.
[16] B. Na, N.N. Tian, R.H. Lv, S.F. Zou, W.F. Xu, Annealing-induced oriented crystallization and its influence on the mechanical responses in the melt-spun monofilament of poly(L-lactide), Macromolecules 43 (2010) 1156–1158.
[17] L. Suryanegara, A.N. Nakagaito, H. Yano, The effect of crystallization of PLA on the thermal and mechanical properties of microfibrillated cellulose-reinforced PLA composites, Compos. Sci. Technol. 69 (2009) 1187–1192.
[18] H. Tsuji, K. Shimizu, Y. Sato, Hydrolytic degradation of poly(L-lactic acid): combined effects of UV treatment and crystallization, J. Appl. Polym. Sci. 125 (2012) 2394–2406.
[19] L.T. Lima, R. Aurasb, M. Rubinob, Processing technologies for poly(lactic acid), Prog. Polym. Sci. 33 (2008) 820–852.
[20] J.J. Hwang, S.M. Huang, H.J. Liu, H.C. Chu, L.H. Lin, C.S. Chung, Crystallization kinetics of poly (L-lactic acid)/montmorillonite nanocomposites under isothermal crystallization condition, J. Appl. Polym. Sci. 124 (2012) 2216–2226.
[21] J.W. Huang, Y.C. Hung, Y.L. Wen, C.C. Kang, M.Y. Yeh, Polylactide/nano- and micro-scale silica composite films. II. Melting behavior and cold crystallization, J. Appl. Polym. Sci. 112 (2009) 3149–3156.
[22] P.J. Pan, B. Zhu, T. Dong, Y. Inoue, Poly(L-lactide)/layered double hydroxides nanocomposites: preparation and crystallization behavior, J. Polym. Sci., Part B: Polym. Phys. 46 (2008) 2222–2233.
[23] H.S. Xu, X. Dai, P.R. Lamb, Z.M. Li, Poly(L-lactide) crystallization induced by multiwall carbon nanotubes at very low loading, J. Polym. Sci., Part B: Polym. Phys. 47 (2009) 2341–2352.
[24] T. Villmow, P. Pötschke, S. Pegel, L. Häussler, B. Kretzschmar, Influence of twin-screw extrusion conditions on the dispersion of multi-walled carbon nanotubes in a poly(lactic acid) matrix, Polymer 49 (2008) 3500–3509.
[25] J.T. Yoon, S.C. Lee, Y.G. Jeong, Effects of grafted chain length on mechanical and electrical properties of nanocomposites containing polylactide-grafted carbon nanotubes, Compos. Sci. Technol. 70 (2010) 776–782.
[26] Z.H. Xu, Y.H. Niu, L. Yang, W.Y. Xie, H. Li, Z.H. Gan, Z.G. Wang, Morphology, rheology and crystallization behavior of polylactide composites prepared through addition of five-armed star polylactide grafted multiwalled carbon nanotubes, Polymer 51 (2010) 730–737.
[27] K. Chrissafis, K.M. Paraskevopoulos, A. Jannakoudakis, T. Beslikas, D. Bikiaris, Oxidized multiwalled carbon nanotubes as effective reinforcement and thermal stability agents of poly(lactic acid) ligaments, J. Appl. Polym. Sci. 118 (2010) 2712–2721.
[28] Y.Y. Zhao, Z.B. Qiu, S.K. Yan, W.T. Yang, Crystallization behavior of biodegradable poly(L-lactide)/multiwalled carbon nanotubes nanocomposites from the amorphous state, Polym. Eng. Sci. 51 (2011) 1564–1573.
[29] Y.T. Shieh, Y.K. Twu, C.C. Su, R.H. Lin, G.L. Liu, Crystallization kinetics study of poly(L-lactic acid)/carbon nanotubes nanocomposites, J. Polym. Sci., Part B: Polym. Phys. 48 (2010) 983–989.
[30] Y.X. Shen, J. Tao, W.J. Ren, J.W. Zhang, Z.G. Jiang, Z.Z. Yu, A. Dasari, Chemical and thermal reduction of graphene oxide and its electrically conductive polylactic acid nanocomposites, Compos. Sci. Technol. 72 (2012) 1430–1435.
[31] Y. Sun, C.B. He, Synthesis and stereocomplex crystallization of poly(lactide) graphene oxide nanocomposites, ACS Macro Lett. 1 (2012) 709–713.
[32] H.S. Wang, Z.B. Qiu, Crystallization behaviors of biodegradable poly(L-lactic acid)/graphene oxide nanocomposites from the amorphous state, Thermochim. Acta 526 (2011) 229–236.
[33] H.S. Wang, Z.B. Qiu, Crystallization kinetics and morphology of biodegradable poly(L-lactic acid)/graphene oxide nanocomposites: influences of graphene oxide loading and crystallization temperature, Thermochim. Acta 527 (2012) 40–46.
[34] N.I. Kovtyukhova, P.J. Ollivier, B.R. Martin, T.R. Mallouk, S.A. Chizhik, E.V. Buzaneva, A.D. Gorchinskiy, Layer-by-layer assembly of ultrathin composite films from micron-sized graphite oxide sheets and polycations, Chem. Mater. 11 (1999) 771–778.
[35] J.H. Yang, C.X. Feng, J. Dai, N. Zhang, T. Huang, Y. Wang, Compatibilization of immiscible nylon 6/PVDF blend using graphene oxides, Polym. Int. (2013), http://dx.doi.org/10.1002/pi.4396 (in press).
[36] M. Avrami, Kinetics of phase change. I, J. Chem. Phys. 7 (1939) 1103–1112.
[37] M. Avrami, Kinetics of phase transition. II. Transformation time relations, J. Chem. Phys. 8 (1940) 212–224.
[38] M. Avrami, Granulation, phase change, and microstructure kinetics of phase change. III, J. Chem. Phys. 9 (1941) 177–184.
[39] D.F. Wu, L. Wu, W.D. Zhou, M. Zhang, T. Yang, Crystallization and biodegradation of polylactide/carbon nanotube composites, Polym. Eng. Sci. 50 (2010) 1721–1733.
[40] Y.Y. Shi, L.N. Shao, J.H. Yang, T. Huang, Y.H. Wang, N. Zhang, Y. Wang, Highly improved crystallization behavior of poly(L-lactide) induced by a novel nucleating agent: substituted-aryl phosphate salts, Polym. Adv. Technol. 24 (2013) 42–50.
[41] J.I. Lauritzen, J.D. Hoffman, Extension of theory of growth of chain-folded polymer crystals to large undercoolings, J. Appl. Phys. 44 (1973) 4340–4353.
[42] Y.T. Shieh, G.L. Liu, Effects of carbon nanotubes on crystallization and melting behavior of poly(L-lactide) via DSC and TMDSC studies, J. Polym. Sci., Part B: Polym. Phys. 45 (2007) 1870–1881.
[43] J.D. Hoffman, J.J. Weeks, X-ray study of isothermal thickening of lamellae in bulk polyethylene at the crystallization temperature, J. Chem. Phys. 42 (1965) 4301–4302.
[44] C.Y. Li, Polymer single crystal meets nanoparticles, J. Polym. Sci., Part B: Polym. Phys. 47 (2009) 2436–2440.
[45] J.Z. Xu, T. Chen, C.L. Yang, Z.M. Li, Y.M. Mao, B.Q. Zeng, B.S. Hsiao, Isothermal crystallization of poly(L-lactide) induced by graphene nanosheets and carbon nanotubes: a comparative study, Macromolecules 43 (2010) 5000–5008.
[46] T.X. Liu, Z.S. Mo, S.E. Wang, H.F. Zhang, Nonisothermal melt and cold crystallization kinetics of poly(aryl ether ether ketone ketone), Polym. Eng. Sci. 37 (1997) 568–575.
[47] Z.B. Qiu, Z.S. Mo, Y.N. Yu, H.F. Zhang, S.R. Sheng, C.S. Song, Nonisothermal melt and cold crystallization kinetics of poly(aryl ether ketone ether ketone ketone), J. Appl. Polym. Sci. 77 (2000) 2865–2871.
[48] E.W. Fischer, H.J. Sterzel, G. Wegber, Investigation of the structure of solution grown crystals of lactide copolymers by means of chemical reaction, Kolloid. Z. Z. Polym. 251 (1973) 980–990.